buildings

MDPI

Article

A Thermal Model for Rural Housing in Mexico: Towards the Construction of an Internal Temperature Assessment System Using Aerial Thermography

Miguel Moctezuma-Sánchez [1], David Espinoza Gómez [2], Luis Bernardo López-Sosa [1,*], Iman Golpour [3], Mario Morales-Máximo [1,4] and Ricardo González-Carabes [1]

[1] Dirección Académica, Universidad Intercultural Indígena de Michoacán, Carretera Pátzcuaro-Huecorio Km3, Pátzcuaro 61614, Mexico; moctezum99@yahoo.com (M.M.-S.); mmoralesmaximo@gmail.com (M.M.-M.); ricardogc@iim.unam.mx (R.G.-C.)
[2] Facultad de Físico-Matemáticas, Universidad Michoacana de Nicolás de Hidalgo, Francisco J. Mújica SN, Ciudad Universitaria, Morelia 58040, Mexico; david.espinosa@umich.mx
[3] Department of Energy Engineering, National Distance Education University, C/Juan del Rosal 12, 28040 Madrid, Spain; igolpour@ind.uned.es
[4] Facultad de Ingeniería en Tecnología de la Madera, Universidad Michoacana de San Nicolás de Hidalgo, Av. Francisco J. Múgica S/N, Edificio "D", Morelia 58040, Mexico
* Correspondence: lbernardo.lopez@uiim.edu.mx

Abstract: Estimating energy flows that affect temperature increases inside houses is crucial for optimizing building design and enhancing the comfort of living spaces. In this study, a thermal model has been developed to estimate the internal temperature of rural houses in Mexico using aerial thermography. The methodology used in this study considered three stages: (a) generating a semi-experimental thermal model of heat transfer through roofs for houses with high infiltration, (b) validating the model using contact thermometers in rural community houses, and (c) integrating the developed model using aerial thermography and Python 3.11.4 into user-friendly software. The results demonstrate that the thermal model is effective, as it was tested on two rural house configurations and achieved an error margin of less than 10% when predicting both maximum and minimum temperatures compared to actual measurements. The model consistently estimates the internal house temperatures using aerial thermography by measuring the roof temperatures. Experimental comparisons of internal temperatures in houses with concrete and asbestos roofs and the model's projections showed deviations of less than 3 °C. The developed software for this purpose relies solely on the fundamental thermal properties of the roofing materials, along with the maximum roof temperature and ambient temperature, making it both efficient and user-friendly for rural community management systems. Additionally, the model identified areas with comfortable temperatures within different sections of a rural community, demonstrating its effectiveness when integrated with aerial thermography. These findings suggest the potential to estimate comfortable temperature ranges in both rural and urban dwellings, while also encouraging the development of public policies aimed at improving rural housing.

Keywords: rural housing; aerial thermography; thermal analysis; efficiency

Citation: Moctezuma-Sánchez, M.; Espinoza Gómez, D.; López-Sosa, L.B.; Golpour, I.; Morales-Máximo, M.; González-Carabes, R. A Thermal Model for Rural Housing in Mexico: Towards the Construction of an Internal Temperature Assessment System Using Aerial Thermography. *Buildings* **2024**, *14*, 3075. https://doi.org/10.3390/buildings14103075

Academic Editor: Pei Huang

Received: 15 August 2024
Revised: 21 September 2024
Accepted: 23 September 2024
Published: 26 September 2024

1. Introduction

The efficient use of energy in buildings plays a crucial role in enhancing both energy efficiency and the thermal comfort of occupants. Buildings account for 15% to 40% of total energy consumption, with heating, ventilation, and air conditioning (HVAC) systems representing a substantial share of this usage [1]. Notably, 50% of the energy used for heating and cooling is sourced from fossil fuels. According to the Energy Information Agency (EIA), residential energy consumption is broken down into 47% electricity, 45% natural gas, 4% propane gas, and 4% kerosene [2]. Furthermore, HVAC systems account

for 40% of the energy consumption in houses and buildings [3]. Implementing bioclimatic design strategies to reduce reliance on HVAC systems can significantly lower energy usage, improve habitability [4,5], and promote more sustainable building practices [6].

Improving the energy efficiency of dwellings requires a comprehensive understanding of local climatic conditions, the thermal properties of the building materials, and the requirements for ventilation and temperature ranges for occupant comfort [7–9]. Various strategies can be employed, such as enhancing insulation to reduce heat transfer through the building envelope [10], using low-emissivity windows [11], and improving solar energy absorption in low-temperature areas [12]. Optimizing dwellings from an energy perspective requires the development of models that can identify thermal behaviors and predict effective improvement strategies [13]. Consequently, energy models that accurately capture the thermal behavior of houses and buildings are essential for guiding energy-efficient designs and retrofits [14,15].

To understand the progression of thermal models used for estimating internal temperatures in dwellings, it is important to consider the development of white-box models. These models are based on fundamental physical principles, such as the laws of thermodynamics and heat transfer, to describe a building's thermal behavior. White-box models require detailed information about the materials, building geometry, environmental conditions, and the interactions between different building components [16,17]. Some research [17] has demonstrated the development of sophisticated models that can accurately predict internal temperatures and thermal resistances by combining physical principles with system identification techniques and statistical methods [7]. In addition, some of these models are now integrated into control systems, utilizing computational fluid dynamics (CFD) simulations and software-based analysis to improve their accuracy and applicability [18,19]. These models have proven to be highly effective and reliable in accurately predicting internal temperatures [20]. However, given the variability of real-world conditions, there has been a growing need to investigate internal temperature behavior through more analytical and experimental approaches. This has led to the development of gray-box models, which rely on precise parameters related to building and climate characteristics [21,22]. Some gray-box models use heat transfer analysis techniques to characterize the thermal behavior of both small and large dwellings, often using electrical circuit analogies [23]. Typically, gray-box models combine experimental data with analytical methods to provide accurate and predictive results.

Previous studies on gray-box models [24] have contributed significantly to the development of thermal analysis and control systems for buildings. For instance, a mathematical model was developed using a system of concentrated parameters to analyze and control thermal behavior. This model facilitates the transient analysis of indoor air in response to fluctuating outdoor temperatures, using Matlab/Simulink software (version R2017a). Later, research [25] introduced a Matlab-based tool for simulating hygrothermal performance and assessing energy efficiency. Other studies [26] have focused on hygrothermal interactions between indoor air and heat transfer through the building envelope, incorporating the main sources of moisture into the model. Moreover, a model was developed for simultaneous control of temperature and humidity [27], resulting in a control strategy that optimizes tracking error while minimizing control effort. These models require detailed instrumental analysis to improve the interaction with the building under study and to propose improvements based on a physical analysis of the infrastructure and the outcomes of models.

With the advancement of computational techniques, black-box models have emerged, including those based on artificial neural networks, which use historical data and known variables to predict internal temperatures [28–30]. More recent developments have enhanced accuracy by combining physical simulations with real-time data [31].

White-, gray-, and black-box models have all contributed valuable insights into estimating internal temperatures in dwellings. These models span a wide spectrum, from theoretical analyses based on fundamental principles of thermal physics to empirical studies

utilizing technical instrumentation and computational analysis, and more recently, sophisticated models driven by artificial intelligence. However, there has been a lack of a systematic approach to integrating complementary processes, such as external temperature analysis. In white-box models, external temperatures are typically sourced from databases, recorded with thermometers in gray-box models, or inferred from computational analyses and specific databases in black-box models. The integration of these models with thermographic techniques remains underexplored, despite the potential for non-invasive, straightforward analysis that offers extensive spectral coverage and comprehensive thermal assessment of walls, floors, and roofs. It is therefore crucial to highlight recent advancements in the use of thermography within various thermal prediction models for dwellings.

The use of thermographic techniques to study thermal phenomena in residential buildings has been extensively explored [32]. For example, heat transfer coefficients have been estimated using thermography, a well-established, non-invasive method for temperature assessment [33,34]. Thermographic techniques have proven effective for this purpose over several years. In addition, infiltration analyses have been conducted using a combination of thermography and numerical interpretation methods, further demonstrating the versatility and precision of these techniques in thermal studies [35]. Analytical prediction models and numerical analyses have also been performed using finite element simulations and tomographic analysis [36]. Several studies have also evaluated HVAC-related phenomena by analyzing thermal patterns of large walls and barriers, along with their construction elements, using thermographic images [37]. These advancements have demonstrated the potential of the thermal models based on thermographic analysis for investigating residential buildings [38,39]. In recent years, the application of thermography to indoor heat transfer phenomena has diversified significantly. Some researchers have explored thermal transmittance estimates using electrical–thermal analogies [40]. Additionally, the thermal performance of buildings under normal operating conditions has been extensively studied using both airborne and ground-based thermography, supported by specialized software for analyzing heat loss through walls and windows [41]. Research on window thermography has led to the development of thermal models capable of estimating internal temperatures with an accuracy of less than one degree Celsius [42]. Other studies have focused on heat flow analysis methods to estimate heat transfer coefficients or thermal conductance of building envelope elements. This includes calculating heat transfer coefficients using thermal imaging cameras and heat flow sensors positioned in small wall elements [43]. Furthermore, studies have compared thermal resistance measurements obtained via aerial thermography with different thermal models of buildings to determine internal temperatures more effectively [44]. However, aerial thermography has primarily been studied for characterizing walls to estimate internal temperatures in buildings or multi-level constructions, which may not always be applicable in all sectors. For instance, in rural areas, houses typically have single-level structures, making ground-based thermography potentially sufficient. Unlike multi-level buildings, aerial thermography is more suitable in the rural sector for analyzing house roofs and internal temperatures. This approach is particularly relevant because rural houses are typically single-level structures without varying heights.

Although these models have been applied to rural dwellings [24], they often pose challenges when estimating the thermal behavior of marginalized populations' dwellings due to their technical complexities. In addition, these models are typically limited to controlled conditions and their predictions rely on numerous variables that cannot always be operated as real experimental models. It is also worth noting that there has been significant development and professional adoption of tools designed to simulate heat, air, and moisture (HAM) conditions for building analysis [45]. Despite this progress, many of these HAM tools for building envelope simulations still need users to input detailed characteristics of the building's interior [45]. This necessity underscores both the interest in and the potential for further research in this area, revealing opportunities to enhance the accuracy and usability of such tools. An area of significant opportunity is the estimation

of internal temperatures through thermographic analysis of residential roofs, which is addressed in this study.

In this study, a thermal model based on fundamental physical principles has been developed. This model estimates the maximum and minimum temperatures inside rural dwellings in Mexico, based on the external roof temperature, measured through aerial thermography, as a primary input. This approach enables the preliminary estimation of areas with comfortable temperature zones within houses by analyzing the roof temperature to infer internal conditions. The primary aim of this research is to estimate the maximum and minimum temperatures inside two types of rural houses using a thermal model that incorporates roof temperature measurements obtained through aerial thermography. From these measurements, comfortable temperature ranges are estimated [8]. The model is specifically designed for rural houses, which often experience high levels of infiltration and lack significant thermal inertia. As such, it is particularly suited for simple rural houses, where it offers practical and effective solutions. By utilizing aerial thermography, this methodology eliminates the need for extensive instrumental equipment for individual cases and highlights a significant advancement in optimizing the measurements of internal temperatures in houses for rural dwellings. The development of this model facilitates the construction of a diagnostic system for assessing comfortable temperatures, utilizing aerial thermography, aimed at enhancing housing analysis in rural areas. This system intends to aid in formulating housing improvement strategies and the development of public policies for better housing management. It also optimizes the use of various types of thermometers, ranging from analog and digital to environmental and contact-based, enhancing the accuracy and applicability of temperature measurements in rural housing research.

In summary, the proposed model is a simplified preliminary version that focuses solely on heat transfer through the roof, excluding factors like thermal inertia and heat transfer through walls or windows. Its primary aim is temperature prediction for diagnostic purposes rather than control. Unlike other studies, this model specifically targets small dwellings to simplify calculations and reduce the need for extensive instrumentation. It relies solely on external roof temperature measurements, which can be estimated using aerial thermography—a method not previously reported in the literature. Future research will aim to incorporate additional effects, such as thermal inertia and heat transfer through windows and walls.

2. Materials and Methods

This work facilitated the development of a thermal model designed to predict the internal temperature behavior of typical houses in rural communities in Mexico, employing aerial thermography. The research focused on a case study in the P'urhépecha Plateau region of western Mexico. The methodology used consists of three primary stages (Figure 1): (a) developing a thermal model based on an energy balance approach for predicting the air volume inside the house, (b) validating the model's predictions through temperature estimation via contact thermometers in a semi-experimental setup, and (c) further validating the model's accuracy through aerial thermography and the subsequent development of user-friendly software designed to facilitate practical applications of the model. This structured approach ensures both the accuracy and usability of the thermal model for predicting internal temperatures in rural houses. The proposed methodology facilitates the development of a thermal model for estimating indoor temperatures in rural dwellings with specific characteristics, focusing on roof temperature. Initially, the model is validated through contact thermometer measurements on the exterior roof and compared with indoor temperature readings obtained from ambient thermometers. Subsequently, the model is analyzed using validated aerial thermography, supplemented by contact thermometers on the exterior roof and indoor ambient thermometers, with data processed using freely available software. Given the model's potential for further enhancement, the methodology

is designed to be cyclical, enabling ongoing refinement and strengthening of the proposal in future research.

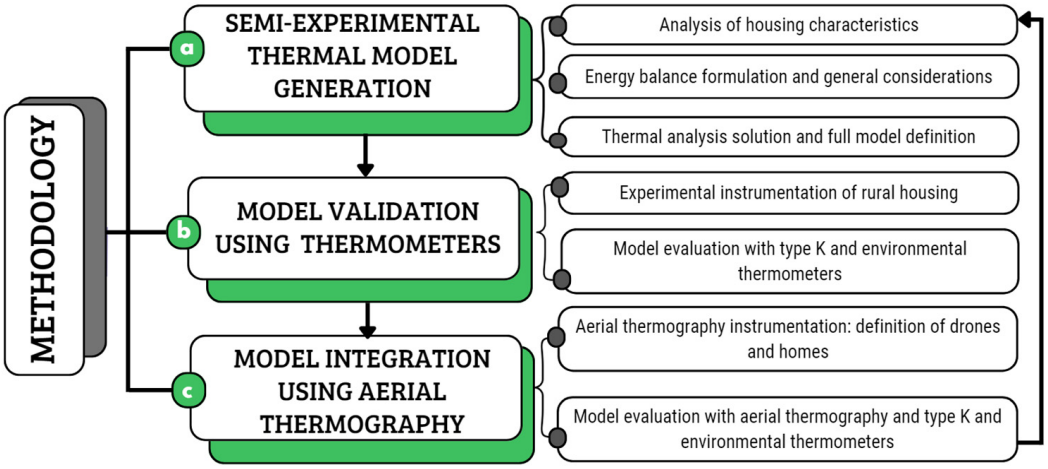

Figure 1. Methodological diagram.

This proposal presents a gray-box model rooted in fundamental energy balance principles and enhanced with experimental data to predict the internal temperature of small, single-story dwellings based on external roof temperature measurements. Unlike similar models examined in previous research [39,41,42], which this study aims to complement, this model uniquely estimates indoor temperatures using external roof temperatures captured via aerial thermography. The following outlines the steps of the proposed methodology.

2.1. Thermal Model

It is important to initially outline all the considerations assumed for the development of the proposed thermal model:

- The roof is regarded as the envelope element receiving the highest solar radiation, leading to higher temperatures compared to other envelope elements. Consequently, it experiences maximum heat transfer [46,47]. Therefore, the model focuses on energy flow through the roof to estimate interior house temperatures, aiming for reliable predictions of indoor temperature. Solar energy absorbed by the roof contributes significantly to temperature increase, forming the basis of the model.
- The current model does not account for the thermal inertia of the roof, despite its recognized importance. The model is simplified to estimate roof temperature based on daily time variations. Future work will include formulations that account for thermal inertia across different roofing materials.
- The thermal analysis is based on a one-dimensional system, providing the foundation framework for the model formulation.
- The model is designed for the analysis of rural housing, where high levels of infiltration are prevalent and challenging to manage. Given this context, thermal inertia is not considered a critical factor in the current analysis.

The energy balance of a house is modeled using a standard cubic framework, incorporating heat transfer through the building envelope, infiltration air flows, and internal heat sources [48,49]. Figure 2a shows the layout of a dwelling and its main energy flows, represented as a basic cubic structure to simplify the analysis. The aim of formulating this simplified model is to determine the internal temperature based on the external roof temperature of the house. Additionally, a specific instrumental design has been used to validate the proposed model, as depicted in Figure 2b.

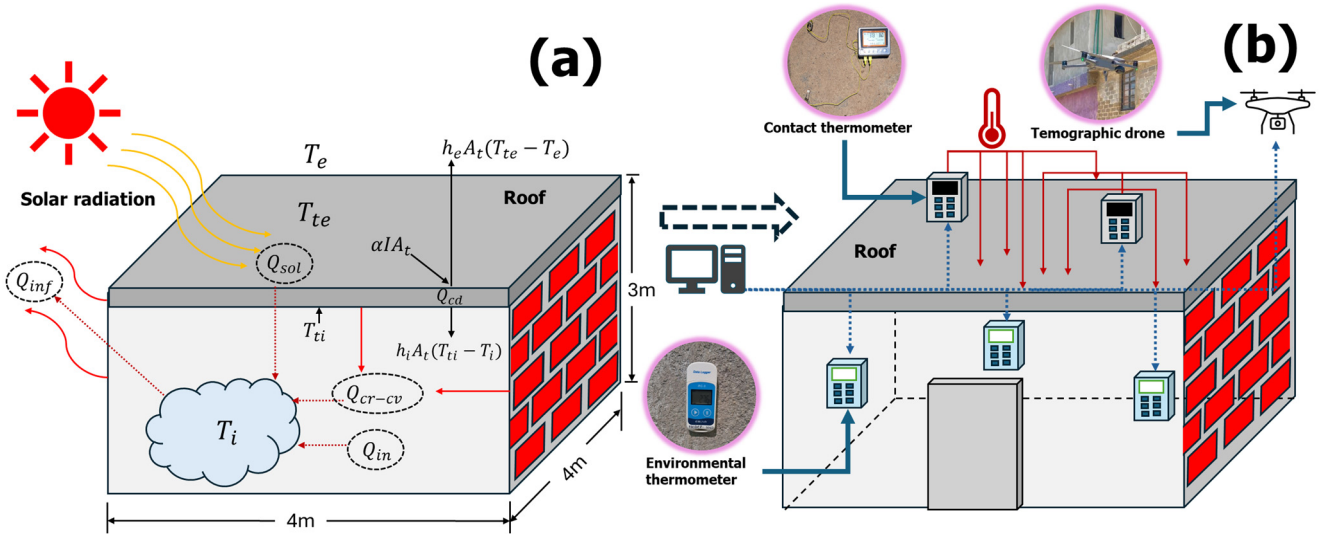

Figure 2. (**a**) Graphical configuration of the proposed energy balance in a house. (**b**) Experimental arrangement for measuring temperatures in a rural house.

As shown in Figure 2a, heat enters the dwelling through the roof and walls via convection and radiation, denoted as Q_{cr-cv} (W). The roof also absorbs a flux of energy from solar radiation, represented as Q_{sun} (W). Additionally, Q_{in} (W) represents the internal heat loads, while Q_{inf} (W) accounts for air infiltration between the inside and the outside of the dwelling. The overall energy balance is then expressed by Equation (1) [49]:

$$V_a \, C_p \rho \, \frac{dTi}{dt} = Q_{in} + Q_{sun} + Q_{cr-cv} - Q_{inf} \tag{1}$$

where V_a is the volume of air (m^3), C_p is the specific heat capacity of air (kJ/kgK), and ρ is the density of air (kg/m^3). The term $\frac{dTi}{dt}$ represents the rate of change of the internal temperature of the dwelling T_i (K) concerning time t. Analyzing the heat flows through the roof, the absorbed solar radiation is given by the expression $\alpha I A_t$, where α is the absorption coefficient, I is the intensity of the solar radiation (W/m^2), and A_t is the area of the roof exposed to the solar radiation (m^2). The total heat Q_e(W) flowing into the roof is the sum of the absorbed solar radiation and the heat entering via convection and radiation, as given by Equation (2):

$$Q_e = Q_{sun} + Q_{cr-cv} = \alpha I A_t + h_e A_t (T_e - T_{te}) \tag{2}$$

In this context, h_e is the combined coefficient of convection and radiation on the exterior of the roof, T_e (K) is the ambient temperature, and T_{te} (K) is the temperature of the external roof surface. The heat conduction Q_{cd} through the roof is given by Equation (3):

$$Q_{cd} = \frac{k \, A_t}{\Delta x} (T_{te} - T_{ti}) \tag{3}$$

Here, k represents the thermal conductivity of the roof material, Δx is the thickness of the roof, and T_{ti} (K) is the internal temperature of the roof. Thus, the convection heat at the inner surface, Q_{c-in} (W), is expressed by applying Equation (4):

$$Q_{c-in} = h_i A_t (T_{ti} - T_i) \tag{4}$$

where h_i is the convection coefficient inside the roof (W/m^2K), and T_i is the indoor air temperature [K]. When treated as a one-dimensional problem, the three heat fluxes—the external heat flux Q_e (W), conduction flux Q_{cd} (W), and convection heat flux at the interior surface Q_{c-in} to the interior air—can be considered equal to a net flux Q_{net}. Thus, we denote the net flux as $Q_{net} = Q_e = Q_{cd} = Q_{c-in}$ (W). This approach, as outlined in refer-

ence [35], is used to calculate the overall transfer coefficient. By solving Equations (2)–(4) simultaneously for $T_e - T_i$, Equation (5) can be obtained as follows [34,35]:

$$T_e - T_i = -\frac{\alpha I}{h_e} + \left(\frac{1}{h_e A_t} + \frac{\Delta x}{k A_t} + \frac{1}{h_i A_t}\right) Q_{net} \tag{5}$$

The sum of the variables, denoted in brackets, refers to the total thermal resistance [50–52] and is measured in (K/W). As shown in Equation (6), this resistance is calculated using Δx, representing the material thickness (m^2), and k, the thermal conductivity of the roofing material (W/mK):

$$R_g = \frac{1}{A_t}\left(\frac{1}{h_e} + \frac{\Delta x}{k} + \frac{1}{h_i}\right) \tag{6}$$

From Equations (5) and (6), Q_{net} (W) is derived as a function of the temperature difference between the exterior and interior environments, accounting for the influence of solar radiation, as expressed in Equation (7):

$$Q_{net} = \frac{\alpha\ I}{R_g h_e} + \frac{(T_e - T_i)}{R_g} \tag{7}$$

By incorporating Q_{net} into both the internal thermal load and the thermal load due to infiltration, the total heat flow, Q_T (W), directed towards the dwelling is obtained, as given in Equation (8):

$$Q_T = Q_{in} + \frac{\alpha\ I}{R_g h_e} + \frac{(T_e - T_i)}{R_g} - Q_{inf} \tag{8}$$

The intensity of direct solar radiation, I (W/m^2), on a horizontal surface can be determined using Equation (9) [53]:

$$I = G_{ND}\sin(\beta) \tag{9}$$

β denotes the solar elevation angle (dimensionless), while G_{ND} represents the clear sky direct solar radiation (W/m^2), both of which can be found in the literature [53].

One notable aspect of the model is its representation of ambient temperature as an analytical function that varies over time. Some researchers have used Equation (10) to model this time-dependent variation in ambient temperature [54–56]:

$$T_e = A + B\sin\left[\frac{\pi(t - b_1)}{b_2}\right] \tag{10}$$

In this equation, t denotes the time of day, while the constants A (K) and B (K) are calculated using Equations (11) and (12) [48]:

$$A = \frac{(T_{max} + T_{min})}{2} \tag{11}$$

$$B = \frac{(T_{max} - T_{min})}{2} \tag{12}$$

where T_{max} (K) represents the maximum temperature observed during the day, and T_{min} (K) corresponds to the minimum temperature, following a pattern similar to the previous scenario. The parameters b_1 (hours) and b_2 (hours) are given in hours and can be calculated using Equations (13) and (14) [56]:

$$b_1 = \frac{(h_{max} + h_{min})}{2} \tag{13}$$

$$b_2 = \frac{(h_{max} - h_{min})}{2} \tag{14}$$

h_{min} (hours) signifies the time at which the minimum temperature occurs, and h_{max} (hours) indicates the time at which the maximum temperature is measured.

Considering the aforementioned approaches, Equation (1) can be reformulated, and Equation (8) can be replaced explicitly with its variables, resulting in an updated energy balance, as shown in Equation (15) [48,49,51]:

$$\rho V_a C_p \frac{dT_i}{dt} = Q_{in} + \frac{(T_e - T_i)}{R_g} + \frac{\alpha\ I}{h_e R_g} - Q_{inf} \tag{15}$$

Rewriting Equation (15) under the assumption of zero infiltration results in Equation (16), which is useful for estimating the maximum thermal load achievable in airtight spaces. In rural dwellings, sleeping areas typically have limited interaction with the external environment, as most daily activities occur in shared spaces like patios and kitchens [57]. In addition, accurately determining all interactions between the house and its surroundings is challenging due to variables like the number of windows and doors and the duration they remain open, which can vary significantly. However, by assuming zero infiltration as an initial approximation, the maximum range of indoor temperatures can still be analyzed effectively for this model.

$$\frac{dT_i}{dt} = b(T_e - T_i) + b\frac{\alpha\ I}{h_e} + bR_g Q_{in} \tag{16}$$

Given that $b = \frac{1}{\rho V_a C_p R_g}$, the units of this parameter are s^{-1}, representing the inverse of time. This parameter can be considered as the relaxation time constant of the thermal system [58]. On the other hand, the temperature of the exterior roof can be obtained using Equation (17) [37]:

$$T_{te} = T_e + \frac{\alpha\ I}{h_e} \tag{17}$$

By isolating the parameter T_e from Equation (17) and substituting it into Equation (16), the differential Equation (18) can be obtained as below:

$$\frac{dT_i}{dt} = b(T_{te} - T_i) + bR_g Q_{in} \tag{18}$$

Considering $Q_{in} \approx 0$ for simplicity, Equation (19) is derived to calculate the interior temperature of the house:

$$\frac{dT_i}{dt} = b(T_{te} - T_i) \tag{19}$$

In this way, the interior temperature is obtained from the temperature of the exterior roof, resulting in the differential Equation (20), as given in Equation (18):

$$\frac{dT_i}{dt} + bT_i = bT_{te} = b\left\{A + B\sin\left[\frac{\pi(t - b_1)}{b_2}\right]\right\} \tag{20}$$

In this context, A and B are constants calculated for the exterior roof temperature, T_{te}. Constant A is related to the average temperature on the outer surface of the roof, while B denotes the amplitude of the temperature variation. The sinusoidal nature of T_{te} is derived from Equation (17), where both T_e and I demonstrate sinusoidal behavior. This sinusoidal estimation of T_{te} as a function of time aligns closely with the experimental observations, as detailed in the results section. The solution of Equation (18) was obtained using the integrating factor method, resulting in Equation (21):

$$T_i = \left\{P\left[B\sin\left(\pi\frac{t - b_1}{b_2}\right)\right] - Q\left[B\cos\left(\pi\frac{t - b_1}{b_2}\right)\right]\right\} + T_0 e^{-bt} + A \tag{21}$$

The parameter T_0(K) is obtained from the initial environmental conditions. The constants P (given by Equation (22)) and Q (given by Equation (23)) are derived by solving Equation (18); these parameters are dimensionless.

$$P = \frac{\left(\frac{b\,b_2}{\pi}\right)^2}{1 + \left(\frac{b\,b_2}{\pi}\right)^2} \tag{22}$$

$$Q = \frac{\frac{b\,b_2}{\pi}}{1 + \left(\frac{b\,b_2}{\pi}\right)^2} \tag{23}$$

2.2. Application of the Thermal Model

To validate the thermal model, roof temperatures were measured for 10 houses—5 with concrete roofs and 5 with asbestos roofs. The average dimensions of the analyzed houses were 4 m in length, 4 m in width, and 3 m in height. Measurements were taken in the municipalities of San Francisco Pichátaro and San Juan Carapan, both located in the state of Michoacán, west of Mexico City. An experimental set-up was established to characterize the temperature both on the roof and inside the house (see Figure 2b). To estimate the roof temperature, two GAIN EXPRESS contact thermometers with 4 type K thermocouples (temperature range: −50~200 °C; accuracy: 0.1 °C) and a Fluke-51-2 Advanced Digital Thermometer were used. Internal temperatures were recorded using 30 thermometers equipped with data loggers and Elitech model RC-5 download software (temperature range: −30 °C to 70 °C; accuracy: ±0.5 °C). Moreover, the validation of the model was conducted using aerial thermography with a MAVIC 3T ENTERPRISE drone equipped with a dual thermal camera (spectral range: 8–14 µm; accuracy: ±2 °C/±2%; measurement range: 0 to 500 °C) and DJI Thermal Analysis Tool 3 software.

Thermographic images were captured in five repetitions per quadrant of the dwellings: covering 2 hectares for groups of dwellings and 0.2 hectares for individual dwellings. For individual houses, aerial photographs were taken from a height of 10 m, while for groups, the height was 60 m. The average roof area of the analyzed dwellings was 20 square meters, and no zoom was applied to any of the aerial images. Emissivity values for aerial thermography were calibrated using contact thermometers to measure roof temperatures, ensuring reproducible measurements and standardizing the reference materials for the roofs. The thermographic images were subsequently analyzed using DJI Thermal Analysis Tool 3 software to estimate the average roof temperatures for each dwelling. These values were manually linked to a custom Python-based software (3.11.4), which integrated the model's algorithm to estimate the internal temperatures of the analyzed dwellings.

2.3. Description of the Case Study

The validation of the proposed model was conducted through experimentation in two indigenous communities located on the P'urhépecha Plateau between March and April, when the average temperature is around 22 °C during spring. According to data from the government of Michoacán, Mexico, this region experiences a predominantly humid temperate and tropical climate, with summer rainfall averaging approximately 1100 mm^3. The region's average minimum temperature is 6 °C, and the average maximum temperature is 25 °C [59]. Situated at an altitude of approximately 1650 m above sea level, the P'urhépecha Plateau provided an ideal setting for testing the model under real-world conditions.

The housing in this region is predominantly rural, with many dwellings lacking basic services such as drainage and piped drinking water. The infrastructure is typically constructed from materials like brick, adobe, wood, metal, or prefabricated components. Roofs are commonly made from galvanized sheeting, black cardboard, clay tiles, asbestos sheets, or concrete. Most houses are single-story and have isolated structures due to the

gradual construction processes in these communities. It is common to find small, separate buildings designated for rooms, kitchens, or bathrooms, often connected by prefabricated materials, known as "corridors".

This research considers these characteristics to propose a thermal model specifically designed for dwellings in this context. To improve accuracy in the initial estimates presented, the model focuses on small, single-story houses, particularly those with concrete roofs and asbestos sheeting. The experimental analyses were carried out from 1 March to 30 April 2024.

3. Results

The most significant findings of the proposed research are outlined below. First, the general weather conditions during the days of the experimental tests are presented. Next, the validation of the proposed model is discussed, comparing it with the experimental temperature measurements taken on the roofs of the studied houses. Finally, the application of the developed methodology is analyzed, which includes temperature measurement via aerial thermography, internal temperature estimation using custom software incorporating the model's algorithm, and an evaluation of its potential application in the rural housing sector.

3.1. Analysis of Meteorological Conditions for Applying the Model

The experimental validation of the model was conducted in two indigenous communities in Michoacán: Pichátaro and Carapan. The experiments were carried out in March and April 2024, under conditions of average solar insolation of 5.2 kWh/m^2 and daytime ambient temperatures peaking at 25 °C. Each community underwent two weeks of measurements. Ten houses were analyzed—those with concrete roofs in April and those with asbestos sheet roofs in March. The ambient temperature was modeled as a sinusoidal function according to Equation (10). Figure 3 illustrates the variations in ambient temperature and solar irradiance throughout a typical day during the measurement period. The graph demonstrates that the modeled ambient temperature closely aligns with experimental measurements, confirming consistency between the theoretical model and the observed results.

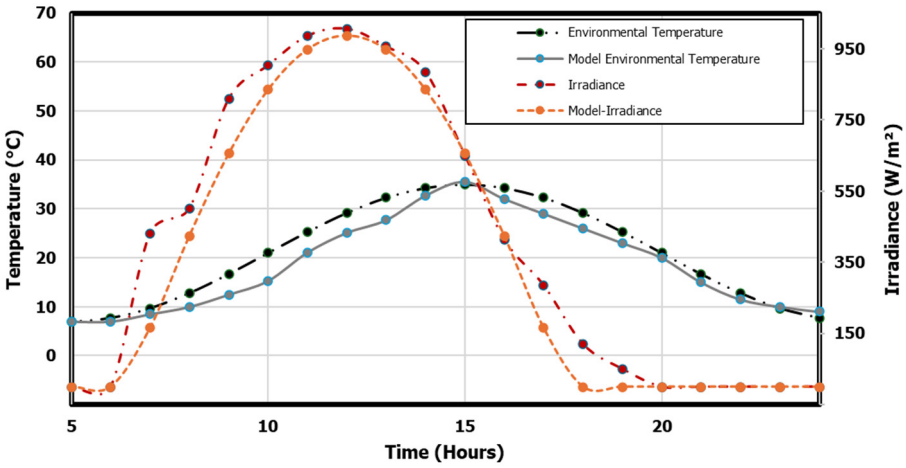

Figure 3. Behavior of the meteorological variables recorded experimentally and compared with the developed model.

During the measurement period, data were collected from a Davis Vantage Pro2 weather station at the Intercultural Indigenous University of Michoacán, located in the study community. The average recorded conditions included a wind speed of 2.2 m/s, cloud cover below 30%, and a relative humidity of 30%. These environmental factors were consistent throughout the measurement days and provided a stable basis for the experimental analysis.

3.2. Model Validation

It should be noted that rural dwellings typically lack the extensive building configurations found in urban areas. In rural regions, construction often occurs in stages and on a relatively small scale. Consequently, the model was developed considering small-scale constructions, using the cubic geometry as a functional approximation due to the typical shape of the houses. Verifying the model, as expressed in Equation (19), required the assessment of the actual conditions of the houses. The constant values of the material properties were sourced from the relevant literature [48,52] and verified with data from suppliers in Mexico [60,61]. These values are presented in Table 1.

Table 1. Properties and parameters used in the analysis.

Material/Coefficient	Thermal Conductivity (W/mK)	Absorption Coefficient	Thickness (m)
Concrete	0.6 [52,61]	0.70 [52,61,62]	0.12 m
Asbestos	0.15 [52,61]	0.75 [52,61,62]	0.0005 m
Constant parameters			
h_e = 13 W/m^{2}K [50]		Air density = 1.2 kg/m^3 [52]	
h_i = 8 W/m^{2}K [50]		Specific heat of air = 1005 J/gK [52]	

The parameters of the model in Equation (19), P and Q, were adjusted to improve the correlation between the model and the experimentally measured indoor temperatures.

Initially, Equation (15) was used to estimate indoor temperatures based on properties of a concrete slab roof during a typical March day. The values of R_g = 0.0312 C/w and b were determined to set parameters P and Q in Equation (15). To improve the model's prediction accuracy, R_g was gradually adjusted under optimal conditions, reducing the prediction error to below 10%. Physically, increasing the thermal resistance R_g reduces heat transfer through the roof, consequently lowering maximum indoor temperatures. Therefore, R_g values significantly depend on roof characteristics. The most accurate predictions of internal temperatures for both concrete and asbestos roofs were obtained with R_g = 0.83 K/W. The model initially failed to predict accurately with the original R_g value, partly due to the omission of thermal inertia of the roof in the model. To address this, the global resistance was adjusted as $R\prime_g = R_g + R_0$, where $R_0 = 0.80$ K/W. The roof temperatures, recorded with the K-type thermocouples, were used to validate the input of the proposed model and compared against indoor temperature measurements taken with environmental thermometers. Figure 4 shows the experimentally recorded daytime temperatures for the roof, T_{tex}, and indoor temperatures, T_{ix}, as well as the model-generated temperatures for the exterior of the roof, T_{te}, and the interior of the dwelling, T_i.

The indoor temperature of a house can vary significantly depending on the size of the individual rooms and the degree of air infiltration caused by windows and doors being left open for different durations. To account for these variables, the experiment was continuously conducted throughout March and April 2024. Figure 4a shows the average thermal behavior of a concrete roof over a typical day in March in a house located in Pichátaro, Michoacán, while Figure 4b displays the corresponding internal temperature of the same house. In April, the experiment was repeated on a typical day, revealing the behavior in a concrete house located in the municipality of Carapan, Michoacán (Figure 4c,d). Figure 4c shows the exterior roof, while Figure 4d depicts the interior of the house. Concrete structures exhibit a slower heating process and a correspondingly slow cooling process. On the other hand, houses with roofs made of asbestos, cardboard, or galvanized sheet metal, exhibit more irregular thermal behavior. Figure 4e,f illustrate the temperature patterns for the roof and interior of a house with an asbestos roof, respectively. These materials tend to have quicker heat absorption and release, leading to more fluctuating temperature patterns compared to concrete structures.

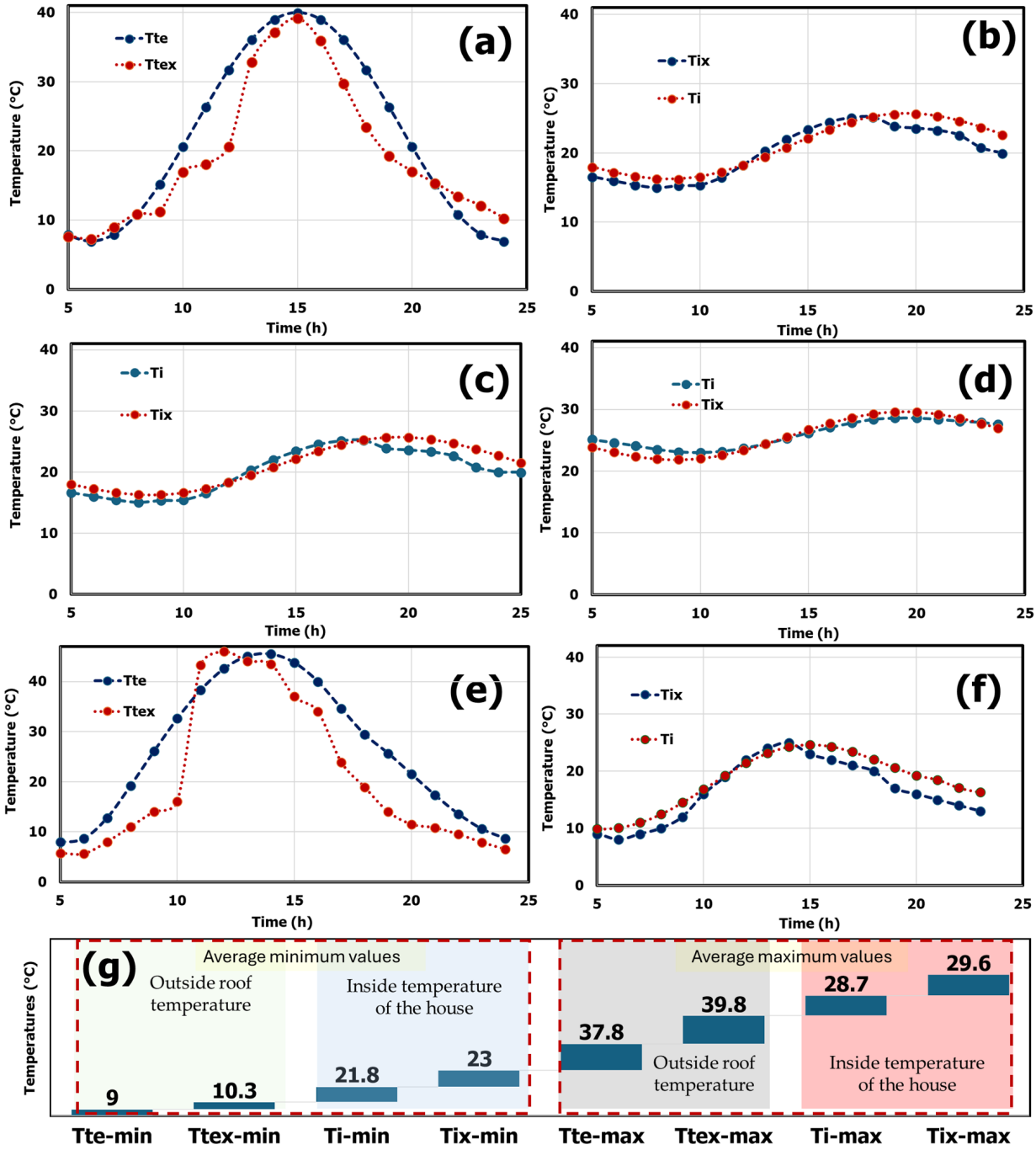

Figure 4. Model validation. Temperature variation in concrete-roofed houses: (**a**) outside during March, (**b**) inside during March, (**c**) outside during April, and (**d**) inside during April. Temperature variation in houses with asbestos sheet roofing: (**e**) outside in March and (**f**) inside in March. (**g**) Average temperature differences between model and experimental data during March and April for concrete-roofed houses.

Temperature variations in 10 houses, comprising 5 with concrete roofs and 5 with asbestos sheets, were analyzed and averaged over the testing months to estimate the maximum and minimum temperature values for both the roof and interior of each house, as shown in Figure 4g. The model demonstrated an average prediction error of 8%, which is considered acceptable with a variation of less than 3 °C. Figure 5a,b show the analyzed house models with concrete roofs and asbestos sheets, respectively.

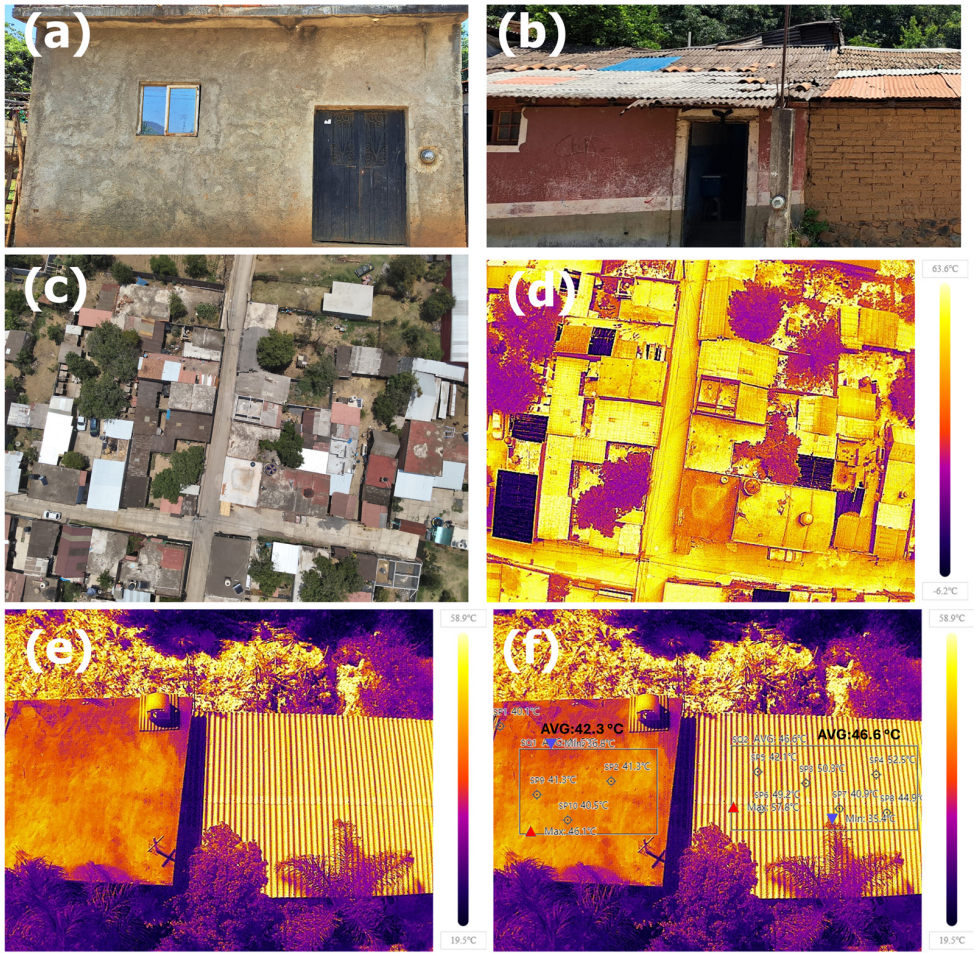

Figure 5. Models of analyzed houses: (**a**) with concrete roofs and (**b**) with asbestos roofs. Thermographic analysis: (**c**) identification of the distribution of houses, (**d**) aerial tomography of the distribution of houses, (**e**) thermography in houses with concrete roofs and asbestos sheets, and (**f**) processing of the thermographic analysis.

On the other hand, within each municipality, there is variation in the housing configurations, which vary mainly in the materials used for the roofs (Figure 5c). The thermographic distribution demonstrating the variety of roof materials is shown in Figure 5d. To validate the model, it was imperative to precisely estimate the temperatures using aerial thermography for houses with both concrete and asbestos roofs, as depicted in Figure 5e. Through image processing techniques, the average temperature distribution within the houses in the case study can be estimated, thus validating the accuracy of the model, as shown in Figure 5f.

The proposed approach integrates the temperatures captured by aerial thermography into the model to predict the indoor temperatures at specific times, on specific days, and in distinct locations. This method eliminates the need for physical entry into the houses and facilitates the generation of optimized scenarios for analyzing acceptable temperature ranges in rural areas, aspects that are being investigated in different parts of the world [39]. In addition, this approach aims to serve as a decision-making tool at a regional level, particularly in areas where indigenous self-governing systems, guided by customs and traditions, manage local public administration resources and generate community plans and strategies [63,64]. To support these local authorities, user-friendly software has been developed, enabling them to conduct the proposed analysis by using aerial thermography data from the houses to predict temperatures within different dwellings. The developed model was also implemented as a computational algorithm using the Python programming language. The source code for solving the posed problem is provided in the Supplementary

Material. Running this code results in an executable file in which users input the study material data through the "main menu". Upon execution, the program produces a graphical analysis of the internal temperature behavior of the house, fulfilling the main objective of the research. The temperature data of the roof were obtained at midday using the DJI Thermal Analysis Tool 3 software and then were entered into the software to estimate the internal temperature of the house.

The Python-based software comprises a main menu featuring three buttons: the first is to access the temperature simulator for the external roof of the house, the second provides access to the temperature simulator for the internal roof of the house, and the third allows exiting the program (see Figure 6a). Upon selecting the "exterior roof temperature" button, a window appears prompting users to input data for the exterior roof, as shown in Figure 6b. These data correspond to the maximum and minimum temperatures of the roof obtained from the analysis of the aerial thermography.

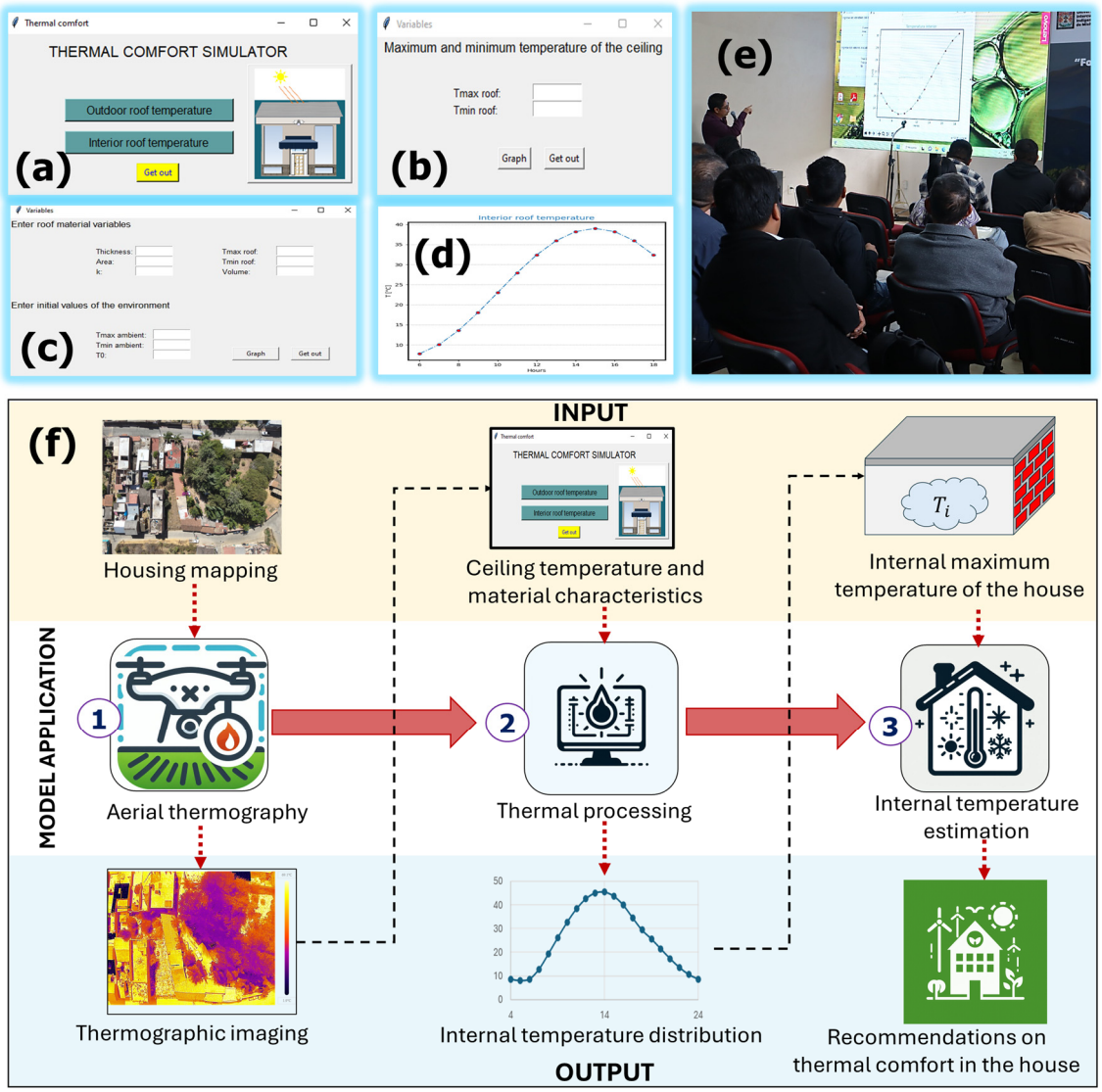

Figure 6. Interface of the developed software: (**a**) main input, (**b**) declaration of temperature variables, (**c**) definition of material properties, and (**d**) results graph. (**e**) Delivery and explanation of the operation of the software. (**f**) Integrated diagram of the application of the thermal model.

The "Roof internal temperature" button displays a section divided into two parts, as depicted in Figure 6c. The first part allows users to input values for the roof material properties such as thermal conductivity (k), area, maximum roof temperature ($T\_max\ roof$),

minimum roof temperature (*T_min roof*), and wall thickness (*Thickness*). The second part is for entering values related to the initial ambient temperature conditions including the maximum and minimum ambient temperatures and the initial temperature (T_0) of the material. Additionally, the interface features two buttons: the "Graph" button, which generates temperature graphs (Figure 6d), and the "Exit" button, which closes the software. The developed software was delivered to the community authorities of the P'urhépecha Plateau in western Mexico to assist in managing community housing plans based on aerial thermography analysis (see Figure 6e). The accessibility of drone technology through the Intercultural Indigenous University of Michoacán, located in the region where these indigenous communities reside, supports this initiative. Furthermore, a comprehensive manual was provided, detailing the methodology for applying the developed model, as illustrated in Figure 6f.

This software generates a graph depicting the internal roof temperature during sunrise and sunset. Furthermore, the descriptive graph provides a straightforward and effective analysis of the numerical estimates, enabling the inference of the internal temperature of a residential house. This information is particularly useful for studying rural dwellings with similar characteristics to those considered in this work.

Figure 5d depicts the behavior of the internal roof temperature during the day in May, represented by a graph showing the average minimum and maximum temperatures analyzed using the DRON ENTERPRISE 3T.

4. Discussion

The model's utility extends beyond being a numerical technical proposal; it serves as a practical tool for designing and managing housing in rural areas, going beyond mere internal temperature estimation. It can be continuously run with initial variables specific to the properties of each material, the characteristics of the houses, and specific locations. It requires two important parameters, namely the minimum and maximum temperature of the house roof, which can be adjusted to determine the internal temperature on the required days (see Figure 7a).

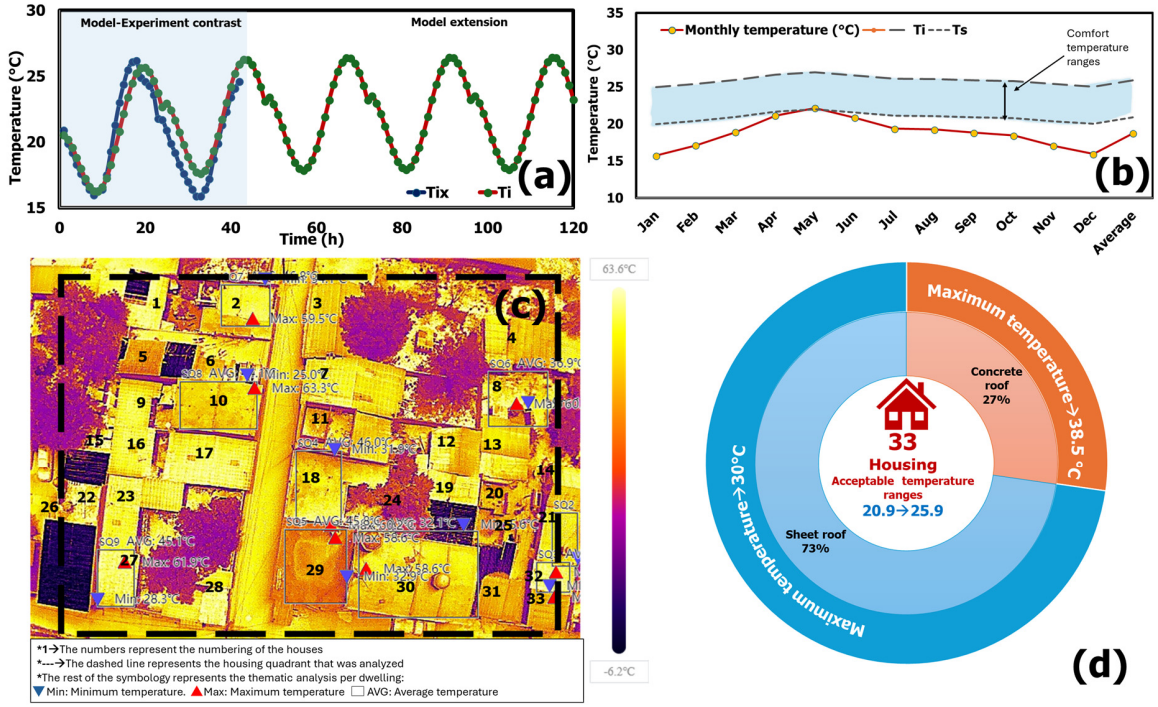

Figure 7. Scope of the thermal model: (**a**) projection of the model with initial data, (**b**) graphical analysis of the comfort temperature range in Pichátaro, (**c**) application of thermographic analysis for estimating comfort temperature ranges, and (**d**) percentage distribution by temperature range of houses.

Provided that the initial conditions remain constant or similar, the model can be extended as needed. This ensures that the results are easily interpretable and applicable in future research. Furthermore, the application of the model is also oriented towards the initial assessment of comfort temperature ranges in rural communities. For instance, in the case of the Pichátaro municipality in Michoacán, it becomes feasible to determine the comfort or neutral temperature ranges conducive to minimizing housing stress [8,65]. This estimation leverages available historical data on average monthly temperatures [66], such as 21.1 °C in April, to project the ideal comfort temperature range for thermally adequate housing. The Auliciems and Szokolay formula [8,65] was used for this calculation, employing Equation (24) to calculate the neutral temperature, thus enabling the derivation of the comfort temperature range in Pichátaro through Equation (25), as illustrated in Figure 7b.

$$T_n = 17.6 + 0.31(T_m) \quad (24)$$

$$Z_n = T_n \pm 2.5\ ^\circ C \quad (25)$$

In this model, T_n represents the neutral temperature, T_m signifies the mean annual or monthly temperature, and Z_n denotes the comfortable temperature zone (°C). In this case, aerial thermography was used to map the distribution of houses in a quadrant of the study community based on roof type (see Figure 7c). An analysis of the temperature distribution categorized houses into two groups: those with concrete roofs and those with sheet roofs (comprising asbestos, cardboard, or tiles). By applying the developed model in this study, the internal temperatures of these houses were estimated, facilitating an analysis of the comfort temperature range. Consequently, it was found that about 30% of the houses with concrete roofs in the analyzed quadrant significantly exceeded the comfort temperature zone, while nearly 70% could potentially achieve comfort temperatures with minimal insulation modifications, as shown in Figure 7d. This example highlights the broad applicability of the proposed research, demonstrating its utility in identifying both potential areas for improvement and the inherent limitations of the current housing structures:

- The thermal model and the software developed are being improved to integrate an analysis with an error of less than 8%. It is expected that statistical data on infiltration can be incorporated in a diagnostic manner, considering the habitability patterns of the inhabitants of rural communities in Mexico. This work is in progress and will be presented in future research.
- In this study, the functionality of the proposed model was validated on both concrete and asbestos roofs. It is important to emphasize the significant differences in the thermal properties of these materials, which influence their performance under different climatic conditions. Concrete roofs, with their higher thermal mass, absorb and store heat during the day and gradually release it at night, helping to stabilize indoor temperature variations. This makes concrete particularly effective in climates with large diurnal temperature swings. In contrast, asbestos slabs, while having a lower thermal mass, provide less insulation and tend to absorb and retain heat, resulting in higher indoor temperatures in hot climates. Due to their limited ability to regulate temperature, asbestos roofs can result in increased energy costs for cooling systems, where available, although air conditioning is rare in rural areas. In addition, the lower thermal conductivity of concrete provides better insulation against external temperature changes than asbestos. The proposed thermal model proves versatility, accurately capturing temperature variations in roofs with rapid temperature changes, such as those with asbestos sheets, as well as roofs with higher heat accumulation and more stable temperatures, such as concrete. This adaptability encourages future research to validate the model with other materials commonly used in rural roofing systems.
- The model currently provides a comprehensive thermal analysis, enabling the examination of thermal comfort temperature ranges within the house. Although the accuracy depends on the assessment of maximum and minimum temperature ranges, the results are sufficiently robust for comparing against the dwelling comfort temperature zones.

- It is important to note that this research provides only an approximation of comfort temperature ranges, referencing historically acceptable ambient temperatures as outlined by Auliciems and Szokolay [8,65], but it does not specifically assess thermal comfort. Instead, the study offers a comparative analysis using a particular frame of reference. Future research will aim to systematically investigate thermal comfort, following specialized standards and procedures to provide a more comprehensive evaluation.
- Future iterations of the model will be accessible to rural communities through a free web platform available in indigenous languages. This platform will include a catalogue of building materials and dimensions for simplified analysis. In addition, an atlas categorizing houses by material type is under development and will be integrated into the platform to further support community-driven assessments.
- The ultimate goal of this initiative is to democratize knowledge and provide universal access to it. The overarching objective is to furnish tools enabling decision making based on analysis and ongoing dialogue with local authorities and members of rural communities. The intention is for the proposal to contribute to the development of housing improvement strategies and management plans at the community level.

The results of the model also revealed some limitations. Given that the type of dwellings studied exhibits a significant amount of uncontrolled infiltration, it is important to note that the exchange of air between the exterior and the interior of the house may diminish the effects of the thermal inertia of both the air volume and the roof [50,67–69]. Additionally, it was found that the shape of the model's temperature curve is sinusoidal, similar to the experimentally measured indoor temperature. This alignment between the predictions and measurements is satisfactory, as the two closely correspond. The results presented here are not universally applicable and may vary in more robust dwellings constructed with higher-quality materials and better insulation, as the thermophysical properties of construction materials and the constantly fluctuating climatic conditions influence the model's performance [67,69]. More elaborately constructed houses, with improved sealing and reduced infiltration, may exhibit different behavior, wherein the thermal mass of the components has a more significant impact. However, the results obtained provide valuable information for the analysis of housing in rural areas with traditional designs, where the proposed model accurately predicts the temperature behavior of such dwellings, which typically experience high levels of uncontrolled infiltration. This serves as an initial proposal, validated through experimental data, and opens opportunities for further research into thermal comfort analysis using thermographic models in rural areas.

After the Python-based software model was delivered to the authorities of the indigenous communities where the study was conducted, it is anticipated that these communities will be able to use it for housing management through their "Public Works Councils" (community offices responsible for managing infrastructure resources). During the software handover, an action plan was outlined to guide how this model can contribute to improving local housing management. Key steps include the following: (a) conducting a thermographic analysis of the entire community to identify areas and dwellings with unfavorable temperature conditions throughout the year, such as low temperatures in winter and high temperatures in summer, while also detecting local heat islands; (b) recommending the gradual replacement of materials that contribute to poor thermal conditions; (c) developing local regulations to ensure that building permits prioritize the use of materials that promote more stable and comfortable temperatures for the community; (d) creating support programs aligned with local, regional, and state public policies to incentivize the adoption of materials that improve indoor thermal conditions for families who otherwise lack access to them; and (e) facilitating multi-sectoral collaboration between the community, academics, organized civil society, and the state government to implement these recommendations and ensure their success. By following this action path, the proposal aims to enhance local hous-

ing conditions and contribute to a more comfortable and sustainable living environment for the communities.

5. Conclusions

The following conclusions are highlighted from this research:

- This research has proposed a thermal model designed to estimate the maximum and minimum temperature ranges inside rural houses, where infiltration is high, and thermal inertia is not considered. The model utilizes roof temperature data obtained through aerial thermography, providing a simple and non-invasive method to analyze the thermal behavior of rural houses in Mexico. The study aims to demonstrate the importance of implementing this thermal model in rural communities, as exemplified by the case study in Pichátaro, Michoacán. This model provides a powerful tool for analyzing and proposing future strategies to improve the comfort temperature range in rural dwellings.
- By integrating historical data, aerial thermography, and the developed model, it is possible to calculate the neutral temperature and the comfort temperature zones. Furthermore, the model facilitates the evaluation of the maximum and minimum internal temperatures within these zones. The initial findings are valuable for identifying the proportion of dwellings that could improve their comfort temperature range with minor modifications, as well as for identifying houses that face habitability challenges due to high internal temperatures.
- The model has some limitations. To date, it has only been applied to small, single-story rural dwellings, specifically in two P'urhépecha communities in western Mexico, and has focused only on houses with concrete and asbestos roofs. As such, there are several areas for further research. Future studies will aim to perform statistical analysis on a wider variety of roofs in more communities with different climatic conditions. In addition, the model will be tested on different roofing materials and extended to a comprehensive analysis of whole communities. The inclusion of more thermal parameters, such as thermal inertia and dynamic heat transfer, will further improve the accuracy of the model and broaden its applicability. These improvements will strengthen the model's predictive capabilities and allow it to address a wider range of housing conditions and materials.
- Moreover, the future availability of the model on a web platform, accessible in indigenous languages and accompanied by an atlas of building materials, will facilitate informed decision making in the formulation of housing management strategies in rural areas. This initiative emphasizes community participation and collaboration with local authorities, holding the potential to transform housing management and comfort in rural communities, thus promoting a sustainable and equitable improvement in the quality of life for their residents.

It is important to mention that the developed model is specifically designed for rural housing and may not be suitable for buildings constructed with sophisticated materials, better thermal insulation, and diverse material configurations. However, it serves as a valuable alternative for the rural sector. Future research aims to expand the model's scope by validating the adjustment constants for different types of housing and materials through statistical analysis. This expansion will involve incorporating thermal inertia, extending the model to include other materials used in housing roofs, and generating a more robust and dynamic analysis. These improvements are expected to decrease the model's error and provide more accurate infiltration estimates across various rural housing types.

Supplementary Materials: The following supporting information can be downloaded at: https://www.mdpi.com/article/10.3390/buildings14103075/s1.

Author Contributions: Conceptualization, M.M.-S. and L.B.L.-S.; methodology, L.B.L.-S.; software, D.E.G.; validation, R.G.-C.; formal analysis, M.M.-S.; investigation, M.M.-S., D.E.G., I.G. and R.G.-C.; resources, L.B.L.-S. and M.M.-M.; data curation, M.M.-S., I.G., M.M.-M. and R.G.-C.;

writing—original draft, M.M.-S., D.E.G. and L.B.L.-S.; writing—review and editing, D.E.G., L.B.L.-S. and I.G.; supervision, M.M.-M. All authors have read and agreed to the published version of the manuscript.

Funding: This research received no external funding.

Data Availability Statement: The data presented in this study are available on request from the corresponding author.

Acknowledgments: The authors would like to thank the postdoctoral fellowship program of the National Council of Humanities, Sciences, and Technologies of the Government of Mexico; the Institute of Science, Technology, and Innovation of the State of Michoacán; the Professional Development Program for Teachers 2023–2024; and the Intercultural Indigenous University of Michoacán for their support in conducting this research. The support from the indigenous communities of the State of Michoacán is also gratefully acknowledged.

Conflicts of Interest: The authors declare no conflict of interest.

Nomenclature

Q_{cr-cv}	Heat transfer by radiation and convection [W].
Q_{sun}	Solar radiation heat [W].
Q_{in}	Internal heat loads [W].
Q_{inf}	Heat due to infiltration [W].
Q_e	External heat flow to the roof [W].
Q_{cd}	Heat flow by conduction [W].
Q_{c-in}	Internal heat flow [W].
h_e	External heat flow coefficient [W/m^2K].
h_i	Internal heat flow coefficient [W/m^2K].
ρ	Density of air [kg/m^3].
C_p	Specific heat of air [J/kgK].
V_a	Volume of air [m^3].
G_{ND}	Clear sky solar radiation [W/m^2].
β	Solar elevation angle [dimensionless].
t	Time of the day [hours].
T_{max}	Maximum exterior temperature [K].
T_{min}	Minimum exterior temperature [K].
b	Time constant of relaxation [s^{-1}].
T_0	Initial temperature [K].
α	Absorption coefficient [dimensionless].
I	Intensity of solar radiation [W/m^2].
k	Thermal conductivity [W/mK].
A_t	Roof area [m^2].
Δx	Rood thickness [m].
T_i	Air interior temperature [K].
T_e	Ambient temperature [K].
T_{te}	Outside roof temperature [K].
T_{ti}	Internal roof temperature [K].
R_g	Total thermal resistance [K/W].
Q_{net}	Net flow due to convection–conduction and solar radiation [W].
Q_T	Total heat flow [W].
A	Mean exterior temperature constant [K].
B	Amplitude of oscillation temperature [K].
b_1	Phase constant [hours].
b_2	Frequency constant [hours].
h_{min}	Hour of minimum exterior temperature [hours].
h_{max}	Hour of maximum exterior temperature [hours].
P	Dimensionless parameter.
Q	Dimensionless parameter.

T_n The neutral temperature [K].
T_m The mean annual or monthly temperature [K].

References

1. González-Torres, M.; Pérez-Lombard, L.; Coronel, J.F.; Maestre, I.R.; Yan, D. A review on buildings energy information: Trends, end-uses, fuels and drivers. *Energy Rep.* **2022**, *8*, 626–637. [CrossRef]
2. Energy Information Administration (EIA). *Annual Energy Outlook*; Energy Information Administration: Washington, DC, USA, 2022; Volume 2022.
3. Australian Government. *Best Practice Maintenance and Operation of HVAC Systems for Energy Efficiency*; Australian Government: Canberra, Australia, 2012.
4. Molina, J.R.; Lefebvre, G.; Gómez, M.M. Study of the thermal comfort and the energy required to achieve it for housing modules in the environment of a high Andean rural area in Peru. *Energy Build.* **2023**, *281*, 112757. [CrossRef]
5. Yuan, T.; Hong, B.; Qu, H.; Liu, A.; Zheng, Y. Outdoor thermal comfort in urban and rural open spaces: A comparative study in China's cold region. *Urban Clim.* **2023**, *49*, 101501. [CrossRef]
6. Perez-Bezos, S.; Grijalba, O.; Hernandez-Minguillon, R.J. Evaluation of Thermal Comfort Perception in Social Housing Context. *Environ. Clim. Technol.* **2023**, *27*, 289–298. [CrossRef]
7. Perera, D.W.U.; Pfeiffer, C.F.; Skeie, N.O. Modelling the heat dynamics of a residential building unit: Application to Norwegian buildings. *Model. Identif. Control* **2014**, *35*, 43–57. [CrossRef]
8. Auliciems, A.; Szokolay, S.V. Thermal comfort. In *Passive and Low Energy Architecture International Design Tools and Techniques*; The University of Queensland: St Lucia, Australia, 1995; pp. 1–69.
9. Çengel, Y.; Boles, M. *Termodinámica*; McgrawHill Interamericana: New York, NY, USA, 2009.
10. Paraschiv, S.; Paraschiv, L.S.; Serban, A. Increasing the energy efficiency of a building by thermal insulation to reduce the thermal load of the micro-combined cooling, heating and power system. *Energy Rep.* **2021**, *7*, 286–298. [CrossRef]
11. Taher, R.; Abdelkader, W.A.; Fahim, A.A.M.A. Sustainable Building: To Achieve Thermal Comfort in Highly Glazed Buildings Using Smart Glass. *IOP Conf. Ser. Earth Environ. Sci.* **2022**, *1113*, 012021. [CrossRef]
12. Lie, B.; Pfeiffer, C.; Skeie, N.-O. Models for solar heating of buildings. In Proceedings of the 55th Conference on Simulation and Modelling (SIMS 55), Modelling, Simulation and Optimization, Aalborg, Denmark, 21–22 October 2014; LiU Electronic Press: Linköping, Sweden, 2014; pp. 21–22.
13. García, Y.; Cuadrado, J.; Blanco, J.M.; Roji, E. Optimizing the indoor thermal behaviour of housing units in hot humid climates: Analysis and modelling of sustainable constructive alternatives. *Indoor Built Environ.* **2019**, *28*, 772–789. [CrossRef]
14. Berthou, T.; Stabat, P.; Salvazet, R.; Marchio, D. Development and validation of a gray box model to predict thermal behavior of occupied office buildings. *Energy Build.* **2014**, *74*, 91–100. [CrossRef]
15. Bacher, P.; Madsen, H. Identifying suitable models for the heat dynamics of buildings. *Energy Build.* **2011**, *43*, 1511–1522. [CrossRef]
16. Arendt, K.; Jradi, M.; Shaker, H.R.; Veje, C.T. Comparative analysis of white-, gray- And black-box models for thermal simulation of indoor environment: Teaching building case study. In Proceedings of the Building Performance Analysis Conference and SimBuild: Co-Organized by ASHRAE and IBPSA-USA, Chicago, IL, USA, 26–28 September 2018; pp. 173–180.
17. François, A.; Ibos, L.; Feuillet, V.; Meulemans, J. Estimation of the thermal resistance of a building wall with inverse techniques based on rapid active in situ measurements and white-box or ARX black-box models. *Energy Build.* **2020**, *226*, 110346. [CrossRef]
18. Das, S.; Subudhi, S. A review on different methodologies to study thermal comfort. *Int. J. Environ. Sci. Technol.* **2022**, *19*, 2155–2171. [CrossRef]
19. Yao, R.; Zhang, S.; Du, C.; Schweiker, M.; Hodder, S.; Olesen, B.W.; Toftum, J.; Romana d'Ambrosio, F.; Gebhardt, H.; Zhou, S.; et al. Evolution and performance analysis of adaptive thermal comfort models—A comprehensive literature review. *Build. Environ.* **2022**, *217*, 109020. [CrossRef]
20. Adilkhanova, I.; Ngarambe, J.; Yun, G.Y. Recent advances in black box and white-box models for urban heat island prediction: Implications of fusing the two methods. *Renew. Sustain. Energy Rev.* **2022**, *165*, 112520. [CrossRef]
21. Li, Y.; O'Neill, Z.; Zhang, L.; Chen, J.; Im, P.; DeGraw, J. Grey-box modeling and application for building energy simulations—A critical review. *Renew. Sustain. Energy Rev.* **2021**, *146*, 111174. [CrossRef]
22. Harb, H.; Boyanov, N.; Hernandez, L.; Streblow, R.; Müller, D. Development and validation of grey-box models for forecasting the thermal response of occupied buildings. *Energy Build.* **2016**, *117*, 199–207. [CrossRef]
23. Bastida, H.; Ugalde-Loo, C.E.; Abeysekera, M.; Qadrdan, M.; Wu, J. Thermal dynamic modelling and temperature controller design for a house. *Energy Procedia* **2019**, *158*, 2800–2805. [CrossRef]
24. Mendes, N.; Oliveira, G.H.; de Araújo, H.X. Building Thermal Performance Analysis By Using Matlab/Simulink. In Proceedings of the Seventh Int IBPSA Conference, Rio Janeiro Brazil, 13–15 August 2001; pp. 473–480.
25. Mendes, N.; Oliveira, G.H.C.; Araújo, H.X.; Coelho, L.S. A MATLAB-based simulation tool for building thermal performance analysis. In Proceedings of the Eighth International IBPSA Conference, Eindhoven, The Netherlands, 11–14 August 2003; pp. 855–862.
26. Holm, A.H.; Künzel, H.M.; Sedlbauer, K. Predicting indoor temperature and humidity conditions including hygrothermal interactions with the building envelope. *ASHRAE Trans.* **2004**, *110 Pt I*, 820–826.

27. Bahramnia, P.; Hosseini Rostami, S.M.; Wang, J.; Kim, G.-j. Modeling and controlling of temperature and humidity in building heating, ventilating, and air conditioning system using model predictive control. *Energies* **2019**, *12*, 4805. [CrossRef]
28. Elbeltagi, E.; Wefki, H. Predicting energy consumption for residential buildings using ANN through parametric modeling. *Energy Rep.* **2021**, *7*, 2534–2545. [CrossRef]
29. Abida, A.; Richter, P. HVAC control in buildings using neural network. *J. Build. Eng.* **2023**, *65*, 105558. [CrossRef]
30. Agouzoul, A.; Simeu, E.; Tabaa, M. Synthesis of model predictive control based on neural network for energy consumption enhancement in building. *AEU-Int. J. Electron. Commun.* **2024**, *173*, 155021. [CrossRef]
31. Elmaz, F.; Eyckerman, R.; Casteels, W.; Latré, S.; Hellinckx, P. CNN-LSTM architecture for predictive indoor temperature modeling. *Build. Environ.* **2021**, *206*, 108327. [CrossRef]
32. Tabet Aoul, K.A.; Hagi, R.; Abdelghani, R.; Syam, M.; Akhozheya, B. Building envelope thermal defects in existing and under-construction housing in the uae; infrared thermography diagnosis and qualitative impacts analysis. *Sustainability* **2021**, *13*, 2230. [CrossRef]
33. Fokaides, P.A.; Kalogirou, S.A. Application of infrared thermography for the determination of the overall heat transfer coefficient (U-Value) in building envelopes. *Appl. Energy* **2011**, *88*, 4358–4365. [CrossRef]
34. Żmudzińska-Nowak, M.; Krause, P.; Krause, M. Infrared thermography of walls in residential buildings in historic workers' housing estates in upper silesia. *Intell. Syst. Control Autom. Sci. Eng.* **2018**, *92*, 257–267. [CrossRef]
35. Lerma, C.; Barreira, E.; Almeida, R.M.S.F. A discussion concerning active infrared thermography in the evaluation of buildings air infiltration. *Energy Build.* **2018**, *168*, 56–66. [CrossRef]
36. Fokaides, P.A.; Jurelionis, A.; Gagyte, L.; Kalogirou, S.A. Mock target IR thermography for indoor air temperature measurement. *Appl. Energy* **2016**, *164*, 676–685. [CrossRef]
37. Al-Kassir, A.R.; Fernandez, J.; Tinaut, F.V.; Castro, F. Thermographic study of energetic installations. *Appl. Therm. Eng.* **2005**, *25*, 183–190. [CrossRef]
38. Georgiou, L.; Stasiuliene, L.; Valancius, R.; Seduikyte, L.; Jurelionis, A.; Fokaides, P.A. Investigation of the performance of mock-target IR thermography for indoor air temperature measurements under transient conditions. *Meas. J. Int. Meas. Confed.* **2023**, *208*, 112461. [CrossRef]
39. Jiang, T.; Hao, F.; Chen, X.; Zou, Z.; Zheng, S.; Liu, Y.; Xu, S.; Yin, H.; Yang, X. Estimating indoor air temperature by obtaining outdoor building window surface temperature using infrared technology: An exploratory approach. *Build. Environ.* **2024**, *251*, 111218. [CrossRef]
40. Patel, D.; Estevam Schmiedt, J.; Röger, M.; Hoffschmidt, B. A Model Calibration Approach to U-Value Measurements with Thermography. *Buildings* **2023**, *13*, 2253. [CrossRef]
41. Moga, L.; Moga, I.; Șoimoșan, T.; Moldovan, I.; Rădulescu, M.; Rădulescu, A.; Iancu, I. Infrared thermography application for in-situ determination of the building envelope thermal performance. *J. Phys. Conf. Ser.* **2023**, *2654*, 012122. [CrossRef]
42. Chen, X.; Zou, Z.; Hao, F.; Wang, Y.; Mei, C.; Zhou, Y.; Wang, D.; Yang, X. Remote sensing of indoor thermal environment from outside the building through window opening gap by using infrared camera. *Energy Build.* **2023**, *286*, 112975. [CrossRef] [PubMed]
43. Danielski, I.; Fröling, M. In situ measurements of thermal properties of building fabrics using thermography under non-steady state heat flow conditions. *Infrastructures* **2018**, *3*, 20. [CrossRef]
44. Memari, X.; Memari, A. Comparative Study of Indoor Infrared Thermography Method to Estimate the Overall Thermal Resistance for Building Envelope Systems. *Int. J. Archit. Eng. Constr.* **2019**, *8*, 14–21. [CrossRef]
45. Foucquier, A.; Robert, S.; Suard, F.; Stéphan, L.; Jay, A. State of the art in building modelling and energy performances prediction: A review. *Renew. Sustain. Energy Rev.* **2013**, *23*, 272–288. [CrossRef]
46. Ran, J.; Tang, M.; Jiang, L.; Zheng, X. Effect of Building Roof Insulation Measures on Indoor Cooling and Energy Saving in Rural Areas in Chongqing. *Procedia Eng.* **2017**, *180*, 669–675. [CrossRef]
47. Ponni, M.; Baskar, R. Evaluation of Indoor Temperature through Roof and Wall Temperatures-An Experimental Study in Hot and Humid Climate. *Certif. Int. J. Eng. Innov. Technol.* **2008**, *9001*, 2277–3754.
48. Duffie, J.A.; Beckman, W.A.; Worek, W.M. *Solar Engineering of Thermal Processes*, 4th ed.; John Wiley & Sons: Hoboken, NJ, USA, 2003; Volume 116. [CrossRef]
49. Chwieduk, D. *Solar Energy in Buildings Thermal Balance for Efficient Heating and Cooling*; Elsevier: Amsterdam, The Netherlands, 2014.
50. Wang, S.K. *Handbook of Air Conditioning and Refrigeration*; McGraw-Hill: New York, NY, USA, 1994; Volume 32.
51. Cao, E. *Heat Transfer in Process Engineering*; McGraw Hill: New York, NY, USA, 2009.
52. Holman, J. Jack Holman—Heat Transfer (2001, McGraw-Hill Science—Engineering—Math). Available online: https://www.scribd.com/document/760152681/Jack-Holman-Heat-Transfer-2001-McGraw-Hill-Science-Engineering-Math-Libgen-lc (accessed on 13 August 2024).
53. Cycles, R.; Comfort, T.; Health, I.E.; Buildings, A.A.; Resources, E.; Information, C.D.; Estimating, E.; Methods, M.; Design, D. *ASHRAE Handbook*; ASHRAE: Peachtree Corners, GA, USA, 1997.
54. Calmon, J.L. Estudio Térmico y Tensional en Estructuras Masivas de Hormigón. Aplicación a Las Presas Durante la Etapa de Construcción. Doctoral's Thesis, Universitat Politécnica de Catalunya, Barcelona, Spain, 1995.

55. Mirambell, E. Criterios de Diseño en Puentes de Hormigón Frente a la Acción Térmica Ambiental. Doctoral Thesis, Universitat Politécnica de Catalunya, Barcelona, Spain, 1987.
56. Emerson, M. *The Calculation of the Distribution of Temperature in Bridges*; Crowthorne: Berkshire, UK, 1973.
57. Torres, E.; Vega, L.M.; Higuera, C. La dimensión socio espacial de la vivienda rural en la ciudad de México: El caso de la Delegación Milpa Alta. *Rev. INVI* **2011**, *26*, 201–223. [CrossRef]
58. Arias, J.; Khan, A.A.; Rodriguez-Uría, J.; Sama, M. Analysis of smart thermostat thermal models for residential building. *Appl. Math. Model.* **2022**, *110*, 241–261. [CrossRef]
59. IPLAEM-Gobierno-Michoacán Región VI Meseta Purepécha: CARPETA DE ESTADÍSTICA BÁSICA 2020. 2021. Available online: http://mapadigital.michoacan.gob.mx/index.php/regional (accessed on 10 July 2024).
60. CEMEX Losa de Concreto. Available online: https://www.cemexmexico.com/ (accessed on 1 December 2022).
61. CYPE-Ingenieros-S.A. Generador de Precios de la Construcción México. Available online: https://mexico.generadordeprecios.info/ (accessed on 2 April 2023).
62. Yao, J.; Yan, C. Effects of solar absorption coefficient of external wall on building energy consumption. *World Acad. Sci. Eng. Technol.* **2011**, *76*, 758–760.
63. Aragon-Andrade, O. La emergencia del cuarto nivel de gobierno y la lucha por el autogobierno indígena en Michoacán, México. *Cah. Des. Amériques Lat.* **2020**, *94*, 57–81. [CrossRef]
64. Leco Tomás, C.; Fuerte García, J.M. Los Autogobiernos Indígenas en la Región Purépecha Hacia un Desarrollo Comunitario. In *El Orden Mundial Reconfigurando las Teorías, las Políticas Públicas Regionales y sus Resultados Migratorios*; UNAM-AMECIDER: Ciudad de México, México, 2022; pp. 341–362.
65. Butera, F.; Fanchiotti, A.; Farruggia, S. *Experimental Validation of a Finite Differences Trombe Wall Model*; Passive and Low Energy Architecture: Pergamon, Turkey, 1983; pp. 629–639. [CrossRef]
66. NASA POWER Data Access Viewer. Available online: https://power.larc.nasa.gov/data-access-viewer (accessed on 23 September 2023).
67. Verbeke, S.; Audenaert, A. Thermal inertia in buildings: A review of impacts across climate and building use. *Renew. Sustain. Energy Rev.* **2018**, *82*, 2300–2318. [CrossRef]
68. Shaviv, E.; Yezioro, A.; Capeluto, I.G. Thermal mass and night ventilation as passive cooling design strategy. *Renew. Energy* **2001**, *24*, 445–452. [CrossRef]
69. Ulgen, K. Experimental and theoretical investigation of effects of wall's thermophysical properties on time lag and decrement factor. *Energy Build.* **2002**, *34*, 273–278. [CrossRef]